ELSEVIER

Chemical Engineering Journal 139 (2008) 245–255

Chemical Engineering Journal

www.elsevier.com/locate/cej

Adsorption of Cr(VI) using thermally activated weed *Salvinia cucullata*

S.S. Baral [a,*], S.N. Das [a], G. Roy Chaudhury [a], Y.V. Swamy [a], P. Rath [b]

[a] *Regional Research Laboratory, Bhubaneswar 751013, India*

[b] *Department of Chemical Engineering, National Institute of Technology, Rourkella 769008, India*

Received 31 August 2006; received in revised form 25 July 2007; accepted 27 July 2007

Abstract

Cr(VI) removal studies were carried out by using activated carbon obtained from waste weed, *Salvinia cucullata*. Effects of various parameters, such as pH, contact time, temperature, adsorbate concentration, adsorbent dose and particle size of the adsorbent on percentage of adsorption were studied. The adsorption studies were carried out at an agitation speed of 600 rpm to minimize the film diffusion. The adsorption kinetics followed dual rate; it was fast during a first stage and then it was reduced. The equilibrium was achieved in 12 h. The kinetics increased with decrease in pH. Adsorbate and adsorbent concentration also influenced the kinetics. The adsorption process was endothermic in nature. The reaction kinetics followed pseudo-second-order kinetic equation. Empirical rate equation developed, which explained the effect of various adsorption parameters, was studied. Theoretical numbers of stages were calculated based on the results. Intra-particle diffusion was found to be the rate-controlling step. Optimization studies were also carried out to establish the upper and lower breakthrough points.

Keywords: Adsorption; Cr(VI); Optimization; Kinetics; Thermodynamics; Column studies

1. Introduction

Due to increase in population coupled with use of various metals in different industrial and household materials, the load of toxic metal pollutants in the environment is increasing. During processing, the waste generated may be either in the form of gas, liquid or solid. The waste from metallurgical/mining sector, in general, creates destabilization in the ecosystem, as most of the heavy metal ions are toxic to all living organisms. Although some of these heavy metals in traces play significant role in human metabolic system, their higher concentrations are toxic. A general awareness has been created regarding development of various adsorbent techniques to treat such effluents. Among the different heavy metals, chromium is a very common pollutant [1]. The sources of chromium contamination in wastewater are electroplating, leather processing, metal finishing industries and chromite mining [2].

In view of the pollution hazards caused by Cr(VI), several methods of removal have been reported including chemical precipitation, reverse osmosis, ion exchange, foam flotation, electrolysis and adsorption. Among all the above-mentioned methods, adsorption is an economically feasible alternative due to easy operation and development of various cheap adsorbents. A variety of materials are used as adsorbent for Cr(VI) and various studies have been published documenting its adsorption on red-mud [2], activated carbon obtained from different waste materials [3,4], biomaterials [5], hydrotalcite [6], chitson [7], goethite [8], bauxite [9], etc. In the present study, the material used, *Salvinia cucullata*, a weed, which grows profusely in sweet water. Here, an attempt was made to prepare activated carbon and to study its feasibility as an adsorbent for removal of Cr(VI) from aqueous solution. Adsorption efficiency was investigated as a function of agitation speed, pH, time, concentration of adsorbate, amount of adsorbent and temperature.

2. Experimental

2.1. Material

All the reagents used in this study were of analytical grade. Aqueous solution of Cr(VI) was prepared by dissolving req-

* Corresponding author. Tel.: +91 9861084217.
E-mail address: ss_baral2003@yahoo.co.in (S.S. Baral).

1385-8947/$ – see front matter © 2007 Elsevier B.V. All rights reserved.
doi:10.1016/j.cej.2007.07.090

uisite amount of $K_2Cr_2O_7$ in double distilled water. A stock solution having concentration 1000 mg/l of Cr(VI) was prepared and subsequently diluted to the required strengths to carry out the adsorption studies. The pH of the solution was varied using dilute hydrochloric acid and sodium hydroxide solutions.

2.2. Adsorbent preparation

S. cucullata, used in this study was collected from a lake situated about 15 km from Bhubaneswar, the capital city of Orissa. The weed grows profusely and is removed periodically to enhance the life of the lake. The weed collected from the lake was washed with tap water followed by distilled water and sun-dried. Drying at 60 °C for 1 h in an oven removed the adhering moisture. The dried material was crushed to powder. The powdered material was transferred to a muffle furnace and activation was carried out at 500 °C under nitrogen atmosphere for 1 h. Subsequently, the carbonized mass was cooled to ambient temperature under nitrogen to prevent complete combustion. The carbonized mass thus produced was ground and sieved to different fractions. Malvern Particle Size Analyzer was used to determine the particle size. The smallest size fraction, i.e., 53.55 μ was used for adsorption studies. The chemical and physical properties of the raw material are shown in the Table 1.

XRD analysis showed the peaks related to the major component corresponding to carbon.

2.3. Adsorption studies

Adsorption studies were carried out in batches using 250 ml of Cr(VI) solution taken in 500 ml beaker and stirred in Rime make mechanical stirrers where the temperature can be maintained within ±0.5 °C of the desired value. For higher temperatures, the adsorption studies were carried out in a sealed unit to avoid the evaporation loss. Five millilitres of representative samples were drawn from the reaction mixture at regular interval and filtered. The residual Cr(VI) concentration was analyzed spectrophotometrically using diphenyl carbazide in a PE LAMBDA 35 UV–vis spectrophotometer [10]. Unless otherwise mentioned, all adsorption studies were carried out under following conditions: pH, 1.7; agitation speed, 600 rpm; adsorbent concentration, 2 g/l; adsorbate concentration, 500 mg/l; temperature, 30 °C; contact time, 12 h. The equilibrium adsorption capacity was calculated using the following equation:

$$q_e = \frac{(C_0 - C_e)V}{M} \quad (1)$$

where q_e is the equilibrium adsorption capacity (mg/g), C_0, C_e are initial and equilibrium concentrations (mg/l) of Cr(VI) in the solution, V is the volume (l) of solution taken and M is the mass (g) of adsorbent used.

Continuous adsorption studies were carried out in a perpex column. The internal diameter and height of the column were 5 and 30 cm, respectively. The Cr(VI) solution was pumped through a metering pump (Watson Marlow make) at the bottom of the column and the effluent was collected from the top. Samples were collected at regular intervals for analysis. The flow rate of solution was checked regularly. The pressure drop was measured through a manometer. The concentration of Cr(VI) in the inlet solution was 500 mg/l and flow rate was 60 ml/min. The adsorption studies continued till there was no difference between inlet and outlet solution.

Table 1
Physico-chemical characteristics of the adsorbent

Parameter	Carbonization temperature			
	400 °C	500 °C	600 °C	700 °C
Volatile matter (%)	34.1	28.4	17	15.6
Ash (%)	45.4	44.3	58.3	58.4
Fixed carbon (%)	20.5	27.3	24.7	22.7
Surface area (m^2/g)	4.26	16.4	44.9	79.2
Particle size (cm)	0.01875	0.01875	0.01875	0.01875
Porosity (%)	46.5	48.9	49.2	49.8
Density (g/cm^3)	1.48	1.44	1.42	1.40
Iodine number	–	1050	–	–
XRD peak	Carbon	Carbon	Carbon	Carbon

3. Results and discussion

3.1. Effect of agitation speed

Adsorption studies were carried out by varying the agitation speed from 100 to 800 rpm to find out the speed at which the liquid boundary layer played insignificant role. The results are shown in Fig. 1. The adsorption efficiency increased with increase in agitation speed upto 600 rpm and thereafter, it attained a steady state. This indicates that the thin liquid film surrounding the adsorbent plays an insignificant role disallowing the adsorbate to reach the adsorbent surface.

3.2. Effect of contact time

Adsorption experiments were carried out over 900 min to find the optimum contact time. The results are shown in Fig. 2. Fig. 2 shows that the kinetics was very fast during the first 30 min,

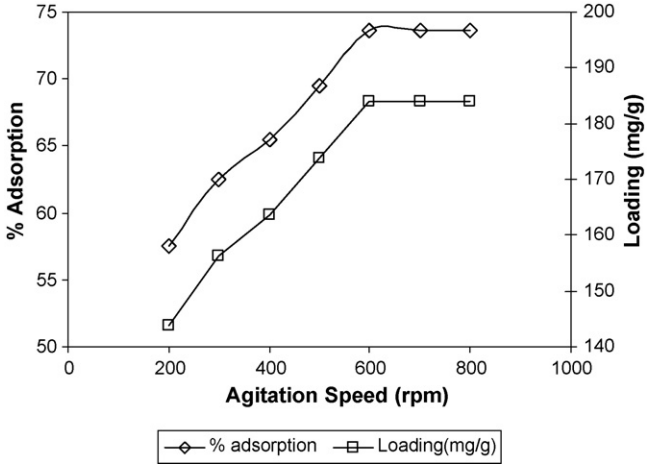

Fig. 1. Effect of agitation speed (conditions: pH, 1.7; temp., 30 °C; adsorbate conc., 500 mg/l; adsorbent dose, 2 g/l; contact time, 12 h; particle size, 53.55 μ).

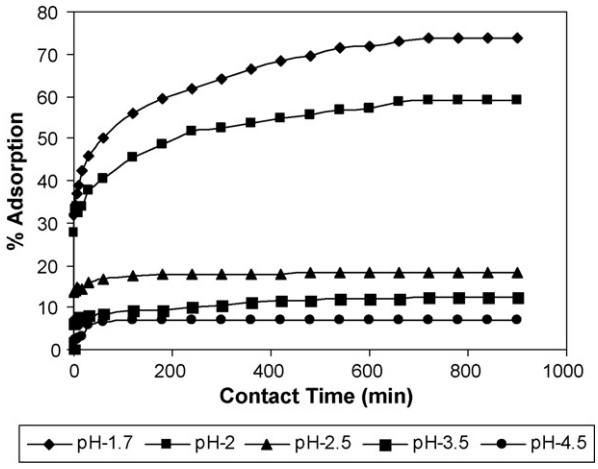

Fig. 2. Effect of contact time (conditions: temp., 30 °C; adsorbate conc., 500 mg/l; adsorbent dose, 2 g/l; stirring rate, 600 rpm; particle size, 53.55 μ).

during this time, the 60% of the total adsorption was reached. This stage was followed by a slower kinetics one. The adsorption reaction attained equilibrium within 12 h and beyond that, there was hardly any change in concentration. Therefore, all further studies were carried out for 12 h. The dual adsorption kinetics may be due to the different mechanisms governing the process. Adsorption of species can takes place only when the adsorbate is transported from bulk to the adsorbent surface. The initial faster rate may be due to surface adsorption and in the initial stage, the surface is free and reaction proceeds at a faster rate. Once the available free surface is clogged, then the adsorbate molecules penetrate through the pores and get adsorbed inside the pore, which is known as intra-particle diffusion. The intra-particle diffusion accounts for slower kinetics at the later step. Similar dual mechanisms are also reported by others [3].

3.3. Effect of pH

The initial pH was varied between 1.7 and 4.5. The results are shown in Fig. 3. It was observed that adsorption efficiency decreased with increase in pH. It was further observed that the equilibrium pH in all cases was higher than the initial pH, which indicates ligand exchange mechanism governing the process. Adsorption may be occurring due to electrostatic force of attraction as well as formation of complex with the chelating agent present in the adsorbent. Evidence of complex formation was obtained from Fourier transform infrared spectroscopy using FT-IR 1600 Perkin-Elmer make. For the FT-IR study, 2 mg of finely ground adsorbent as well as Cr(VI)-loaded materials were mixed separately with 400 mg of KBr (spectroscopy grade) and pressed to prepare translucent sample disks. Results show that the adsorbent contain two or more functional groups. The bands at 1100 and 1700 cm^{-1} in the pure adsorbent correspond to C–O and C=O stretching frequencies representing carbonyl and carboxyl groups. Several peaks were also observed around 3500 cm^{-1} for anion groups present [11]. The Cr(VI)-loaded materials showed either shift or reduction in adsorption peak suggesting the vital role played by the functional groups. The XRD analysis of the adsorbent showed the *d*-values 3.16, 2.84, 2.01 and 1.45 corresponding to carbon. The peak intensity decreased after adsorption indicating the reaction between carbon matrixes with the anion.

3.4. Effect of initial Cr(VI) concentration

The initial Cr(VI) concentration was varied from 400 to 700 mg/l to evaluate its effect on adsorption efficiency. It is observed that with the increase in initial concentration of Cr(VI), the percentage of adsorption decreases as is generally expected in the equilibrium process. Adsorption increases from 58.6 to 78.12% when the initial adsorbate concentration decreases from 700 to 400 mg/l as shown in Fig. 4. The metal ion uptake capacity, which is defined as the milligram of adsorbate adsorbed per gram of adsorbent, shows a reverse trend. The uptake capactiy increases from 156.24 to 205.11 mg/g when the initial Cr(VI) concentration goes up from 400 to 700 mg/l. This may be due to higher metal ion concentration enhancing the driving force to overcome mass transfer resistance between the aqueous and

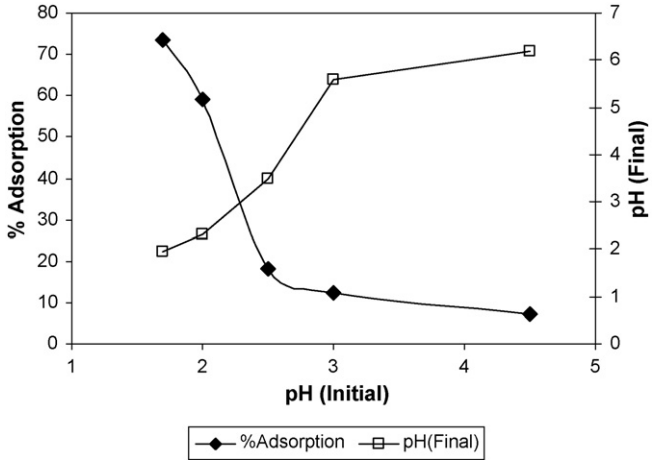

Fig. 3. Effect of pH (conditions: temp., 30 °C; adsorbate conc., 500 mg/l; adsorbent dose, 2 g/l; contact time, 12 h; stirring rate, 600 rpm; particle size, 53.55 μ).

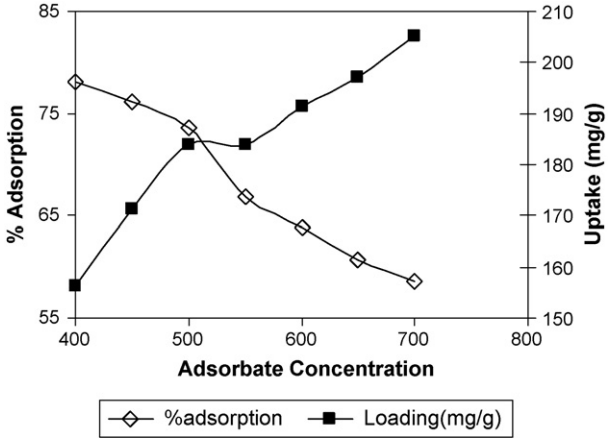

Fig. 4. Effect of initial Cr(VI) concentration (conditions: pH, 1.7; temp., 30 °C; adsorbent dose, 2 g/l; contact time, 12 h; stirring rate, 600 rpm; particle size, 53.55 μ).

solid phases resulting in higher probability of collision between adsorbate molecules and adsorbent surface.

3.5. Effect of adsorbent concentration

Adsorbent concentration was varied from 0.8 to 2.4 g/l to find its effect on the adsorption efficiency. It is observed that the uptake decreases from 247.35 to 167.93 mg/g when the adsorbent concentration increases from 0.8 to 2.4 g/l. The percentage of adsorption increases from 39.58 to 80.61 when the adsorbent concentration increases from 0.8 to 2.4 mg/l. The results are shown in Fig. 5. Higher percentage of adsorption with the increase of adsorbent concentration may be due to the availability of more surface area. The decrease in Cr(VI) uptake at higher adsorbent dose may be due to competition of the Cr(VI) ions for the adsorption sites available. Further agglomeration of the adsorbent particle may be another possible reason of the decrease in uptake.

3.6. Effect of temperature

Temperature is an essential parameter in the kinetics study as the wastewater temperature varies widely. The temperature was varied from 30 to 60 °C and the results are shown in Fig. 6. The percentage of adsorption and uptake increase from 54.7 to 76.5 and 136.75 to 191.25 mg/g, respectively, when the temperature increases 30–60 °C. The increase in efficiency with increase in temperature indicates that the reaction followed endothermic pathway. The enhancement in the adsorption efficiency with increase of temperature may be due to various factors such as enhancement of inter-reaction between adsorbent and adsorbate and creation of new adsorption sites [12].

3.7. Effect of particle size of adsorbent

The particle size of adsorbent was varied from 53.55 to 312.76 μ to evaluate the effect of particle size on adsorption. The results are shown in Fig. 7. The percentage of adsorption decreases from 73.6 to 39.5 when the particle size increases from 53.55 to 312.76 μ, while the uptake decreases from 184 to 98.75 mg/g under same conditions. The decrease in percentage adsorption as well as uptake with increase in particle size may be attributed to the decrease in specific surface area of the adsorbent.

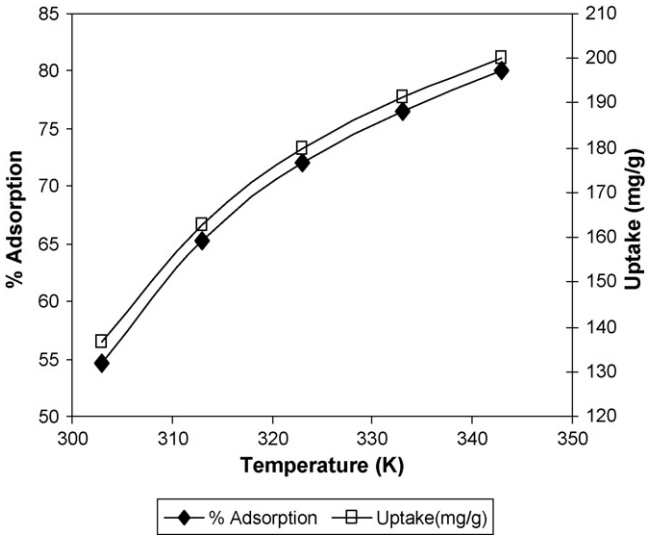

Fig. 6. Effect of temperature (conditions: pH, 1.7; adsorbate conc., 500 mg/l; adsorbent dose, 2 g/l; contact time, 12 h; stirring rate, 600 rpm; particle size, 53.55 μ).

From the above studies, it can be concluded that three parameters, such as pH, time and adsorbate concentration determine the kinetics of adsorption. The adsorbent concentration is not considered as it plays an insignificant role when up-flow reactor is employed. In case of batch experiments, the adsorbate concentration was kept constant because of which maximum loading could not be observed. But in case of up-flow reactor, new adsorbent particles continuously come in contact with the adsorbate ions. So maximum loading (mg of adsorbate per g of adsorbent) was found to be independent of the adsorbent dose, i.e., bed height in this case. So adsorbent dose plays insignificant role in case of column studies.

3.8. Evaluation of rate equation

In order to determine a suitable kinetics model, the adsorption rate is fitted into four kinetic equations such as—

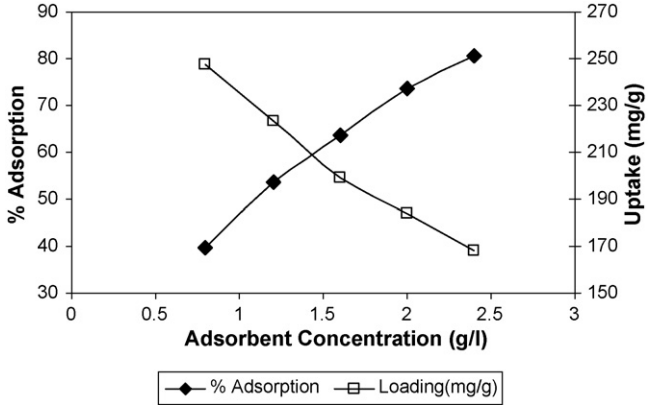

Fig. 5. Effect of adsorbent dose (conditions: pH, 1.7; temp., 30 °C; adsorbate conc., 500 mg/l; contact time, 12 h; stirring rate, 600 rpm; particle size, 53.55 μ).

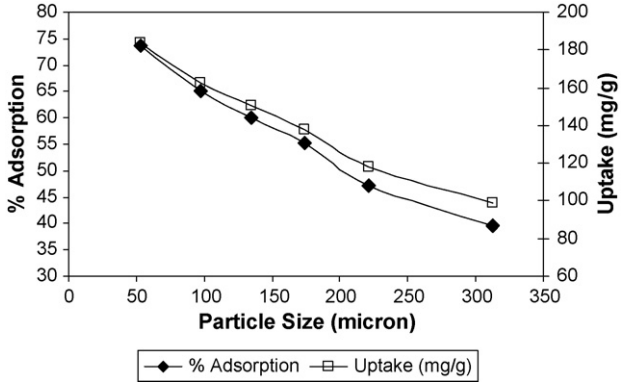

Fig. 7. Effect of particle size (conditions: pH, 1.7; temp., 30 °C; adsorbate conc., 500 mg/l; adsorbent dose, 2 g/l; contact time, 12 h; stirring speed, 600 rpm).

(a) Pseudo-first-order.
(b) First-order reversible.
(c) Ritchie second-order.
(d) Pseudo-second-order.

(a) Pseudo-first-order:

$$\log(q_{eq} - q_t) = \log q_{eq} - \frac{k_1 t}{2.303} \quad (2)$$

where 'q_{eq}' is the amount of solute adsorbed at equilibrium per unit mass of adsorbent (mg/g), 'q_t' is the amount of solute adsorbed at any given time 't' and 'k_1' the rate constant.

(b) First-order reversible:

$$\ln(1 - U_t) = -k_r t \quad (3)$$

where U_t is the fractional attainment of equilibrium and is given by

$$U_t = \frac{C_{A0} - C_A}{C_{A0} - C_{Ae}}, \qquad K_c = \frac{C_{Be}}{C_{Ae}} = \frac{k_1}{k_2}, \qquad k_r = k_1 + k_2$$

where K_c is the equilibrium constant and C_{Ae} and C_{Be} are the equilibrium concentrations. k_1 and k_2 are the first-order rate constants. C_A and C_{A0} (mg/l) are the concentration at time 't' and initial concentrations of adsorbate, respectively.

(c) Ritchie second-order:

$$\frac{q_e}{q_e - q_t} = 1 + k_2 t \quad (4)$$

where k_2 is the Ritchie's reaction rate constant.

(d) Pseudo-second-order:

$$\frac{t}{q_t} = \frac{1}{k q_e^2} + \frac{1}{q_e} t = \frac{1}{h} + \frac{1}{q_e} t \quad (5)$$

where $h = k q_e^2$ and is known as initial sorption rate while k is the second-order rate constant.

Table 2 shows the reaction rate constant along with R^2 values. From R^2 and equilibrium concentration values for different adsorption parameters, it can be concluded that the adsorption process follows pseudo-second-order kinetics.

The initial adsorption kinetics depends on adsorption parameters like initial pH, particle size, adsorbent and adsorbate concentrations. Therefore, the rate equation can be written as:

$$\text{Rate} = \frac{-dC}{dt} = k_u (\text{pH})_1^n (\text{particle size})_2^n (\text{adsorbate})_3^n (\text{adsorbent})_4^n \quad (6)$$

where C = Cr(VI) concentration.By converting equation to logarithmic form:

$$\log(\text{rate}) = \log k_u + n_1 \log(\text{pH}) + n_2 \log(\text{particle size}) + n_3 \log(\text{adsorbate concentration}) + n_4 \log(\text{adsorbent concentration}) \quad (7)$$

To determine the order of reaction, experimental data obtained are arranged to fit into Eq. (7). For this purpose, only one parameter was varied keeping all other parameters constant. Since specific initial rate is proportional to the rate of the reaction, to evaluate the rate order, the respective specific rate is plotted against the percentage adsorption. Using the n and $\log k$ values from the Arrhenius equation, the rate equation can be written as

$$\log(\text{rate}) = \frac{-7.1732 - 1.5677}{T - 2.92 \log(\text{pH})} - 0.2266 \log(\text{particle size}) + 0.9278 \log(\text{adsorbate concentration}) - 0.3895(\text{adsorbent concentration}) \quad (8)$$

3.9. Evaluation of thermodynamic parameters

The activation energy (E) for Cr(VI) adsorption can be calculated by using Arrhenius equation

$$\ln k = -\frac{E}{RT} + \ln A_0 \quad (9)$$

where k = rate constant, A = frequency factor; R = universal gas constant.

By plotting $\ln k$ versus $1000/T$, the activation energy can be calculated from the slope. The activation energy was found to be 13.033 kJ/mol. The low activation energy indicates that physical forces govern the adsorption.

The standard free energy change (ΔG^0) was calculated by using the following relationship:

$$\Delta G^0 = -RT \ln b \quad (10)$$

where b = Langmuir constant, T = absolute temperature and R = universal gas constant.

The other thermodynamic parameters, such as change in standard enthalpy (ΔH^0) and standard entropy (ΔS^0) were determined using the following equation:

$$\ln k = \frac{\Delta S^0}{R} - \frac{\Delta H^0}{T} \quad (11)$$

ΔS^0 and ΔH^0 are obtained from the slope and intercept of the Vant Hoff's plot of $\ln k$ versus $1/T$ (figure not shown). The calculated ΔH^0 and ΔS^0 values are 1.57 kJ/mol and 59.64 J/mol, respectively. The positive values of enthalpy indicate the endothermic nature of the reaction. The positive value of ΔS^0 show the increasing randomness at the solid–liquid interface of Cr(VI) ions on the adsorbent.

3.10. Evaluation of rate-determining step

Due to porous nature of the adsorbent used in this study, pore diffusion is also expected in addition to surface adsorption. The contact time variation experiment can be used to study the rate-determining step in the adsorption process [13]. Since the particles were agitated at a speed of 600 rpm, it can be safely assumed that the rate is not limited by mass transfer from

Table 2
Adsorption kinetic model

Parameters	First-order reversible					Pseudo-first-order reversible		Ritchie second-order		Pseudo-second-order reversible		
	k_r	K_C	k_1	k_2	R^2	k	R^2	k_2	R^2	h	k_2	R^2
pH												
1.7	0.0054	1.393	0.00314	0.00226	0.96	0.0053	0.961	0.0832	0.623	0.108	0.00028	0.995
2	0.0049	0.725	0.00206	0.00284	0.93	0.00484	0.93	0.0717	0.529	0.1082	0.00044	0.997
2.5	0.0087	0.111	0.00087	0.00783	0.92	0.00875	0.922	1.2916	0.631	0.0633	0.00765	1
3	0.0053	0.0704	0.00035	0.00495	0.96	0.0053	0.96	0.0852	0.662	0.6443	0.00167	0.994
4.5	0.0076	0.039	0.00028	0.00732	0.89	0.0076	0.89	0.2658	0.722	0.5842	0.00522	1
Adsorbate concentration (mg/l)												
400	0.0047	1.7852	0.003	0.0017	0.95	0.00484	0.949	0.0555	0.553	0.1458	0.0003	0.994
450	0.0048	1.5932	0.003	0.0019	0.95	0.00484	0.954	0.0558	0.604	0.1232	0.00029	0.995
500	0.0054	1.3934	0.0031	0.0023	0.96	0.0053	0.961	0.0832	0.623	0.108	0.00028	0.995
550	0.005	1.0096	0.0025	0.0025	0.95	0.00507	0.951	0.052	0.623	0.224	0.00014	0.979
600	0.0049	0.8817	0.0023	0.0026	0.93	0.00484	0.932	0.0615	0.471	0.1437	0.0002	0.992
650	0.0047	0.7704	0.0021	0.0027	0.93	0.00484	0.929	0.0562	0.488	0.1313	0.00021	0.992
700	0.0042	0.7078	0.0017	0.0025	0.94	0.00415	0.94	0.0346	0.634	0.1342	0.00019	0.991
Adsorbent concentration (mg/g)												
0.8	0.005	0.8187	0.0023	0.0028	0.94	0.00507	0.936	0.0771	0.509	0.0818	0.00021	0.995
1.2	0.0045	0.9652	0.0022	0.0033	0.95	0.00438	0.954	0.045	0.637	0.1103	0.00019	0.992
1.6	0.0045	1.0914	0.0024	0.0022	0.96	0.00461	0.955	0.0451	0.649	0.1315	0.00021	0.992
2	0.0054	1.3934	0.0031	0.0023	0.96	0.0053	0.961	0.0832	0.623	0.108	0.00028	0.995
2.4	0.0053	1.7317	0.0034	0.0019	0.95	0.0053	0.95	0.0897	0.487	0.1182	0.0003	0.996
Particle size (μ)												
54	0.0054	1.3934	0.0031	0.0023	0.961	0.0053	0.961	0.0832	0.623	0.108	0.00028	0.995
98	0.006	0.9321	0.0029	0.0031	0.972	0.00599	0.972	0.0997	0.571	0.1711	0.00022	0.994
135	0.0065	0.7528	0.0028	0.0037	0.963	0.00645	0.963	0.1682	0.497	0.1419	0.00031	0.997
174	0.0065	0.6156	0.0025	0.0040	0.973	0.00645	0.973	0.1527	0.503	0.1842	0.00028	0.994
221	0.0062	0.4466	0.0019	0.0043	0.967	0.00622	0.967	0.1234	0.511	0.2333	0.00031	0.993
313	0.0049	0.3265	0.0012	0.0037	0.95	0.00484	0.95	0.057	0.524	0.2609	0.00041	0.994
Stirring rate (rpm)												
600	0.0054	1.3934	0.0031	0.0023	0.965	0.0053	0.961	0.0832	0.623	0.108	0.00028	0.995
500	0.0056	1.1393	0.003	0.0026	0.953	0.00553	0.953	0.1001	0.505	0.1291	0.00026	0.994
400	0.0056	0.9493	0.0027	0.0029	0.955	0.00553	0.955	0.0943	0.505	0.1499	0.00026	0.993
300	0.0056	0.8333	0.0026	0.0031	0.956	0.00553	0.956	0.09	0.505	0.1693	0.00025	0.993
200	0.0055	0.6765	0.0022	0.0033	0.958	0.00553	0.958	0.0828	0.505	0.2116	0.00023	0.991
Temperature (K)												
303	0.0047	0.6038	0.0018	0.0029	0.943	0.00484	0.942	0.1541	0.327	0.2461	0.00021	0.993
313	0.0055	0.9368	0.0027	0.0028	0.945	0.00553	0.945	0.0982	0.528	0.1666	0.00022	0.996
323	0.0059	1.2857	0.0033	0.0026	0.968	0.00599	0.968	0.0843	0.764	0.1083	0.00028	0.998
333	0.0057	1.6277	0.0035	0.0022	0.947	0.00576	0.947	0.1088	0.492	0.1316	0.0002	0.997
343	0.0051	2.000	0.0034	0.0017	0.959	0.00507	0.959	0.0693	0.679	0.1017	0.00024	0.998

the bulk to the external surface of the particle. Therefore, the rate-determining step may be either surface or intra-particle diffusion. As they happen simultaneously, the slower one of the two stages would be the rate-determining step. The intra-particle diffusion rate varies with the square root of time [3] as shown below

$$q_t = k_{id} t^{1/2} \tag{12}$$

where q_t = amount adsorbed (mg/g), t = time (min) and k_{id} = intra-particle diffusion coefficient (mg/g min$^{1/2}$).

The k_{id} values are determined from the slope of the linear plot between q_t versus $t^{1/2}$ and the result for different experiments are shown in Table 3. From R^2 values, it can be concluded that the process is pore diffusion controlled.

The initial curved portion of the curve (Fig. 2) relates to the surface diffusion (D_1) and the linear portion represents the intra-particle diffusion (D_2) within the adsorbent. Assuming spherical geometry of the adsorbent particles, the relationship between weight uptake and time using Fick's law can be shown as:

$$\frac{q_t}{q_e} = 6\left(\frac{D_1}{\pi a^2}\right)^{1/2} t^{1/2} \tag{13}$$

D_1 can be calculated from the slope of the plot between q_t/q_e versus $t^{1/2}$ for the initial curved portion. For calculation of D_2, following equation can be used,

$$\ln\left(1 - \frac{q_t}{q_e}\right) = \ln\left(\frac{6}{\pi^2}\right) - \left(\frac{D_2 \pi^2 t}{a^2}\right) \tag{14}$$

Table 3
Mass transfer model parameters

Parameter	k_{id}	R^2	$D_1 \times 10^{-12}$	R^2	$D_2 \times 10^{-12}$	R^2
pH						
1.7	3.0447	0.985	0.1167	0.9809	0.3926	0.9477
2	2.1376	0.9051	0.0544	0.7581	0.3271	0.8866
2.5	0.1407	0.646	0.0449	0.8499	0.4871	0.9445
3	0.5313	0.9734	0.0689	0.899	0.4071	0.9696
4.5	0.0768	0.8926	0.7158	0.8314	0.3489	0.9695
Adsorbate concentration						
400	2.8013	0.9948	0.1036	0.9882	0.3344	0.9195
450	2.9152	0.9883	0.0861	0.9874	0.3344	0.9334
500	3.0447	0.985	0.1167	0.9809	0.3927	0.9477
550	4.91	0.9867	0.3668	0.868	0.3998	0.9356
600	3.7981	0.9749	0.0912	0.9113	0.3489	0.8736
650	3.6162	0.9863	0.1594	0.9385	0.3344	0.8624
700	3.5691	0.9692	0.0504	0.9025	0.2835	0.8858
Adsorbent concentration						
0.8	3.9915	0.9953	0.1046	0.9207	0.3635	0.8975
1.2	4.1303	0.9853	0.0265	0.7629	0.3199	0.9332
1.6	3.922	0.9953	0.0673	0.9856	0.3344	0.9342
2	3.0447	0.985	0.1167	0.9809	0.3926	0.9477
2.4	2.7831	0.9739	0.0593	0.9864	0.3780	0.9163
Particle size						
54	3.0447	0.985	0.0018	0.9809	0.39257	0.9477
98	3.3456	0.9735	0.0075	0.9916	1.45064	0.9515
135	2.5855	0.9536	0.0167	0.9864	2.9594	0.9334
174	2.6898	0.9636	0.0296	0.8073	5.14344	0.9572
221	2.27	0.9779	0.0423	0.9914	7.802	0.9388
313	1.8916	0.9731	0.0471	0.9643	11.6008	0.9047
Stirring speed						
600	3.0447	0.985	0.1167	0.9809	0.3926	0.9477
500	3.1162	0.9878	0.1289	0.9767	0.4144	0.9263
400	3.1162	0.9878	0.1452	0.9767	0.4144	0.9263
300	3.1162	0.9878	0.1594	0.9767	0.4144	0.9263
200	3.1162	0.9878	0.1884	0.9767	0.4144	0.9263
Temperature						
30	2.7842	0.9919	0.0319	0.9211	0.3635	0.9209
40	2.7354	0.9895	0.0585	0.9942	0.4071	0.9012
50	2.6027	0.9777	0.245	0.9835	0.6979	0.9747
60	3.018	0.9954	0.2554	0.9974	0.4071	0.9043
70	2.7021	0.9868	0.0917	0.8903	0.3344	0.9562

D_2 can be calculated from the slope of the curve between $\ln(1 - q_t/q_e)$ versus t. The values of D_1 and D_2 for different adsorption parameters are shown in Table 3. From Table 3, it is observed that the D_1 values are always less than that of the D_2 values. So it can be concluded that the surface diffusion is the rate controlling mechanism, as it is the slowest rate. A similar study has been reported by Karthikeyen et al. [3] for Cr(VI) adsorption using activated carbon. With increase in stirring speed, both D_1 and D_2 values were increased.

3.11. Adsorption isotherm

Experimental data are fitted to different isotherm models such as Freundlich, Langmuir and Temkin adsorption isotherms. The linearized form of the three different isotherms are shown below.

Freundlich isotherm

$$\ln q_e = \ln k_f + b_f \ln C_e \tag{15}$$

where k_f = adsorption capacity and b_f = empirical parameter.

Langmuir adsorption isotherm

$$\frac{C_e}{q_e} = \frac{1}{Q^0 b} + \frac{C_e}{Q^0} \tag{16}$$

where Q^0 = adsorption capacity and b = empirical parameter.

Temkin isotherm

$$q_e = \left(\frac{RT}{b}\right) \ln A + B \ln C_e \tag{17}$$

where A and B are constants and characteristics of the process.

The results are shown in Table 4. The average absolute percentage deviations are also included in Table 4, which are

Table 4
Adsorption isotherm

Parameters	Langmuir isotherm						Freundlich adsorption isotherm						Temkin adsorption isotherm					
	Q_0	b	R^2	$(q_e)_{Exp}$	$(q_e)_{cal}$	%Desv.	b_f	k_f	R^2	$(q_e)_{Exp}$	$(q_e)_{cal}$	%Desv.	A	b	R^2	$(q_e)_{Exp}$	$(q_e)_{cal}$	%Desv.
pH																		
1.7	16.75	0.0063	0.75	184	85.75	23.42	−1.71	959339	0.9005	183.982	205.068	25.8	0.0018	−18.63	0.991	183.982	193.01	12.953
2				147.9	73.81					147.919	96.4559					147.919	134.64	
2.5				45.42	27.27					45.4214	28.9624					45.4214	41.552	
3				30.86	26.18					30.8564	25.7125					30.8564	32.342	
4.5				17.94	25.38					17.9363	23.2857					17.9363	24.671	
Adsorbate concentration																		
400	227.3	0.0264	1	156.2	158.6	1.887	0.193	68.422	0.9142	156.241	161.973	1.97	1.1966	71.763	0.925	156.241	161.66	1.9706
450				171.3	168					171.255	168.517					171.255	168.81	
500				184	176.6					183.982	175.33					183.982	175.95	
550				183.9	188.1					183.917	186.548					183.917	187.14	
600				191.4	193.5					191.438	192.966					191.438	193.24	
650				197.1	197.9					197.083	199.164					197.083	198.94	
700				205.1	201					205.106	204.005					205.106	203.27	
Adsorbent concentration																		
0.8	322.6	0.0102	0.99	247.3	243.4	2.611	0.34	35.009	0.9867	247.35	243.888	1.2192	0.1089	35.942	0.973	247.35	242.42	1.8579
1.2				223.6	226.4					223.612	222.84					223.612	224	
1.6				199.1	209.2					199.105	205.076					199.105	207.03	
2				184	184.9					183.982	184.078					183.982	184.98	
2.4				167.9	160.1					167.928	165.744					167.928	163.56	
Particle size																		
54	73.53	0.0107	0.96	184	253.4	11.92	−0.74	7161.7	0.9499	183.982	194.864	4.2023	0.0012	−24.33	0.983	183.982	188.79	2.4126
98				162.7	158.8					162.717	158.571					162.717	160.16	
135				150.2	138.7					150.223	143.662					150.223	146.44	
174				138	126.4					137.957	131.878					137.957	134.55	
221				118	114					117.95	116.817					117.95	117.71	
313				98.75	106.5					98.75	105.68					98.75	103.79	
Stirring speed																		
600	106.4	0.0171	0.99	184	191.2	−0.59	−0.51	2295	0.9873	183.982	185.985	0.924	0.0008	−29.61	0.995	183.982	185.15	0.6129
500				173.8	172.7					173.75	172.694					173.75	173.02	
400				163.8	161.1					163.75	162.083					163.75	162.64	
300				156.3	154.7					156.25	155.275					156.25	155.61	
200				143.8	146.9					143.75	145.589					143.75	145.07	
Temperature																		
303	108.7	0.0198	0.99	136.8	139.9	4.8	−0.46	1723.7	0.9703	136.75	140.661	2.159	0.0007	−32.28	0.986	136.75	139.91	1.493
313				163	153.1					163	158.888					163	160.28	
323				180	170					180	175.681					180	177.08	
333				191.3	190.6					191.25	190.496					191.25	190.62	
343				200	219.6					200	205.234					200	203.09	

calculated for each isotherm at different parameters according to the following equation:

$$\%\text{Desv.} = 100 \times \frac{1}{N}\sum_{i=1}^{N}\left|\frac{(q_e)_{exp} - (q_e)_{pred}}{(q_e)_{exp}}\right|_i \quad (18)$$

where $(q_e)_{exp}$ and $(q_e)_{pred}$ are the experimental and predicted equilibrium adsorption capacity (mg/g) of the adsorbent, respectively. It is concluded from %Desv. and R^2 values that the isotherm model can be explained by Temkin model. The b_f values are found to be between 0.1 and 1, which proved that the reaction is favorable.

The number of stages/batch reactor required for removal of Cr(VI) was calculated from equilibrium curve [14] obtained from the plot between experimental C_e and q_e values at 35 °C and pH 1.7. The operating line was drawn which was passing through the point (C_0 500 mg/l, q_0 0.0 mg/g) and having slope V_0/X_0 is −1/2 where V_0 is the volume of solution used (0.25 l) and X_0 is the mass of the adsorbent (0.5 g) taken for the adsorption studies. Fig. 8 shows the adsorption isotherm. From Fig. 8, it can be concluded that in three stages the Cr(VI) concentration can be reduced from 500 to <1 mg/l in three stages.

3.12. Factorial design and optimization of parameters

In order to obtain the optimum conditions for adsorption of Cr(VI) on the treated weed, a full factorial design of the type n^k has been used, where n = number of levels and k = number of factors under verification. Here, time, pH and temperature are chosen as three independent factors/variables ($k = 3$ and $n = 2$) and the percentage of adsorption as the dependent out-

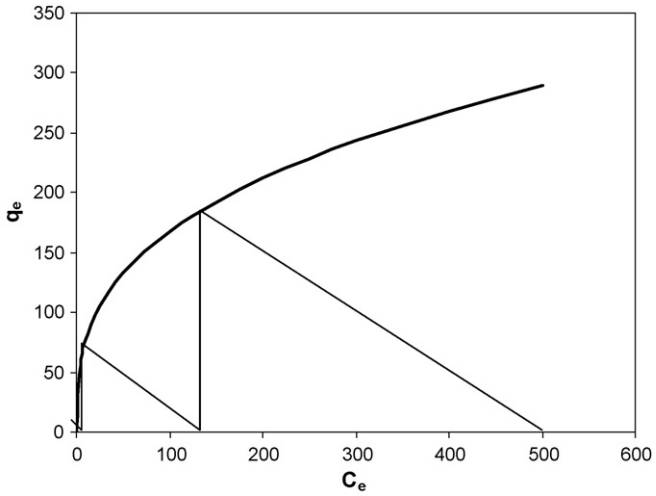

Fig. 8. Number of stages.

put response variable. A 2^3 full-factorial experimental design [15] with number of 3 triplicates at the center point and thus a total of 11 experiments were employed in this study. For statistical calculation of the base level, which is the average of the two levels are calculated using the following relation:

$$x_i = \frac{(X_i - X_0)}{\delta X} \tag{19}$$

The behavior of the system was explained by the following equation

$$Y = b_0 + b_1x_1 + b_2x_2 + b_3x_3 + b_{12}x_1x_2 + b_{23}x_2x_3 + b_{31}x_3x_1 + b_{123}x_1x_2x_3 \tag{20}$$

where $b_0, b_1, \ldots, b_{123}$ are the regression interaction coefficients of the concerned variables and x_1, x_2 and x_3 are the dimensionless coded factor affecting the process. Here x_1 = time, x_2 = pH and x_3 = temperature. The factorial levels and variation interval of the coded factor are shown in Table 5.

The parameters varied are time (5–15 min) pH (1.6–1.8) and temperature (30–40 °C). The variable parameters in two levels, their coded values and the condition for the base level experiments are given in Table 6. The +, − and 0 designations are given to the higher, lower and base levels, respectively. The coefficients are calculated using the following equation:

$$b_j = \frac{1}{N}\sum_{i=1}^{N} x_{ij}Y_i \tag{21}$$

Table 5
Factorial levels and variation intervals

Factors	−1	0	1	Variation interval
x_1	5	10	15	5
x_2	1.6	1.7	1.8	0.1
x_3	30	35	40	5

x_1 = Time in min, x_2 = pH and x_3 = temperature in °C

Table 6
Design of trial runs (in coded form) for adsorption of Cr(VI)

Trial no.	x_1	x_2	x_3	x_1x_2	x_2x_3	x_3x_1	$x_1x_2x_3$	Y
1	+	+	+	+	+	+	+	38.84
2	−	+	+	−	+	−	−	35.94
3	+	−	+	−	−	+	−	51.13
4	−	−	+	+	−	−	+	45.95
5	+	+	−	+	−	−	−	35.38
6	−	+	−	−	−	+	+	27.03
7	+	−	−	−	+	−	+	41.43
8	−	−	−	+	+	+	−	35.43
9	0	0	0	0	0	0	0	27.14
10	0	0	0	0	0	0	0	27.1
11	0	0	0	0	0	0	0	27.15

where 'i' and 'j' are the number of rows and columns, respectively. The "b" values are obtained by using experimental results in the regression Eq. (21). Putting the 'b' values, Eq. (20) becomes

$$Y = 38.89 + 2.8x_1 - 4.593x_2 + 4.074x_3 + 0.0088x_1x_2 - 0.981x_2x_3 - 0.784x_3x_1 - 0.579x_1x_2x_3 \tag{22}$$

The significance of each coefficient was assessed using the Student's t method [17] and the insignificant terms were neglected from Eq. (20). Fisher's adequacy test [16] at 99% confidence level was used to test the regression equation and it was observed that the following equation was adequate:

$$Y = 38.89 + 2.8x_1 - 4.593x_2 + 4.074x_3 - 0.981x_2x_3 \tag{23}$$

From the factorial design, the optimum adsorption parameters obtained are time = 10 min, pH = 1.7 and temperature = 35 °C.

3.13. Column studies

Up-flow column studies were conducted at optimum parameters, such as retention time, 10min; pH, 1.7; temperature, 35 °C obtained form the factorial design method to evaluate Cr(VI) removal from the solution using the prepared adsorbent. The column contains 50 g of material. The lower breakthrough point was obtained at an effluent concentration of 0.1 mg/l (Cr(VI)), as it is the permissible limit for drinking water [17]. The higher breakthrough point relates to complete saturation of the adsorbent material. The number of bed volume is defined as the volume of solution treated/volume of adsorption bed. The lower and higher breakthrough points are observed to be 210 and 1220 bed volume for initial Cr(VI) concentration of 100mg/l at an initial pH of 1.7. The value of 210 bed volume at lower breakthrough point indicates that the material is suitable to treat Cr(VI) contaminated water. The higher breakthrough point was observed to be 1220, which indicates the maximum uptake value to be 156 mg/g of adsorbate.

The adsorption capacity of the present adsorbent was compared with other similar adsorbents for Cr(VI) reported in literature. The comparison is shown in Table 7, from which it can

Table 7
Comparison with other adsorbents

Adsorbent	Uptake capacity	pH	Initial concentration (mg/l)	Reference
Aeromonas cavae	124.46	2.5	5–350	[11]
Chlorella vulgaris	24	2	25–250	[18]
Zooglera ramigera	3	2	25–400	[18]
Halimeda opuntia	40	4.1	25–400	[18]
Rhizopaus arrhizus	62	2	25–400	[19]
Rhizopaus arrhizus	8.8	2		[18]
Rhizopaus nigrificans	123.45	2	50–500	[20]
Sargassum	40	2		[21]
Spirogira	14.7	2	25	[22]
Pinus sylvestris	201.81	1	50–300	[23]
Hazelnut shell activated carbon	170	1	1000	[24]
Tyres activated carbon	58.50	2	60	[25]
Coconut shell carbon	20	2	–	[26]
Coconut shell carbon	10.88	4	25	[27]
Sawdust activated carbon	44.05	2	200	[3]
Thermally activated weed	247	1.7	500	Current study

be concluded that the present adsorbent is efficient in treating Cr(VI) contaminated water.

4. Conclusions

The activated carbonized biomass was found to be a good adsorbent for Cr(VI). Results showed that the initial part of the adsorption process confined only to surface adsorption and the slower kinetics may be due to intra-particle diffusion. The pseudo-second-order kinetics could explain the observed data. The adsorption isotherm followed Temkin model. From the adsorption isotherm curve, the theoretical number stages were determined to reduce the Cr(VI) concentration to the predetermined level. The FTIR showed the anionic bonding with the chelate forming part of the adsorbent. Optimization studies were also carried out by varying only three parameters such as pH, contact time and temperature to find out the significant factor by the help statistical technique. Column studies were also carried out to evaluate the suitability of the adsorbent in treating Cr(VI) contaminated water and the maximum uptake of Cr(VI) observed to be 156 mg/g of the adsorbent at a flow rate of 3.6 l/h, pH 1.7, biomass weight 50 gm and adsorbate concentration 100 mg/l.

Acknowledgements

The authors are thankful to Director, Regional Research Laboratory, Bhubaneswar for his encouragement and permission to publish. One of the author (SSB) thanks CSIR, New Delhi for providing financial assistance.

References

[1] G.S. Agarwal, H.K. Bhuptawat, S. Chaudhari, Biosorption of aqueous Cr(VI) by Tamarinds indica seed, Bioresour. Technol. 97 (2006) 949–956.
[2] J. Pradhan, S.N. Das, R.S. Thakur, Adsorption of Cr(VI) from aqueous solution by using activated red mud, J. Colloid Interface Sci. 217 (1999) 137–141.
[3] T. Karthikeyen, S. Rajgpal, L.R. Miranda, Cr(VI) adsorption from aqueous solution by *Hevea brasilinesis* saw dust activated carbon, J. Hazard. Mater. 124 (1–3) (2005) 192–199.
[4] K. Mohanty, M. Jha, B.C. Meikap, M.N. Biswas, Biosorption of Cr(VI) from aqueous solutions by Eichhornia crassipes, Chem. Eng. J. 117 (2006) 71–77.
[5] N. Tewari, P. Vasudevan, B.K. Guha, Study on biosorption of Cr(VI) by *Mucor hiemalis*, Biochem. Eng. J. 23 (2005) 185–192.
[6] N.K. Lazarides, D.D. Asouhidou, Kinetics of sorptive removal of Cr(VI) from aqueous solution by calcined Mg-Al-CO_3, Water Res. 37 (2003) 2875–2882.
[7] S. Hasan, A. Krishnaiah, T.K. Ghosh, D.S. Viswanath, V.M. Bodh, E.D. Smith, Adsorption of Cr(VI) on chitosan-coated perlite, Sep. Sci. Technol. 38 (2003) 3775–3793.
[8] M. Lehmann, A.I. Zouboulis, K.A. Matis, Modeling the sorption of metals from aqueous solutions on goethite fixed-beds, Environ. Protect. 113 (2001) 121–128.
[9] M. Erden, H.S. Altundogan, F. Tumen, Removal of hexavalent chromium by using heat-activated bauxite, Miner. Eng. 17 (2004) 1045–1052.
[10] C. Li, H. Chn, L. ZuohuM, Adsorptive removal of Cr(VI) be Fe-modified steam exploded wheat straw, Process Biochem. 39 (2004) 541–545.
[11] M.X. Loukidou, A.I. Zouboulis, T.D. Karapantsios, K.A. Matis, Equilibrium and kinetic modeling of Cr(VI) biosorption by *Aeromonas caviae*, Colloids Surf. A: Physicochem. Eng. Aspects 242 (2004) 93–104.
[12] C. Namasivayam, R.T. Yamuna, Adsorption of Cr(VI) by a low cost adsorbent: biogas residual slurry, Chemosphere 30 (1995) 561–578.
[13] B.S. Inbaraj, N. Suluchana, Basic dye adsorption on a low cost carbonaceous sorbent, kinetics and equilibrium studies, Ind. J. Chem. Tan. 9 (2002) 201–208.
[14] Z. Aksu, T. Kutsal, A bioseparation process for removing lead(II) ions from waste water by using *C. vulgaris*, J. Chem. Technol. Biotechnol. 52 (1991) 109–118.
[15] R.H. Mayer, D.C. Montgomery, Response Surface Methodology, second ed., Wiley, 2002.
[16] S. Akhnazarova, V. Katarov, Experimental Optimization in Chemistry and Chemical Engineering, vol. 151–161, MIR Publisher, Moscow, 1982, pp. 300–330.
[17] S. Devy, R. Bai, Removal of trivalent and hexavalent chromium with aminated polyacrylonitrile fibers: performance and mechanism, Water Res. 38 (2004) 2424–2432.
[18] F. Veglio, F. Beolcini, Removal of metals by biosorption: a review, Hydrometallurgy 44 (1997) 301.
[19] S. Prakasan, J.S. Merre, R. Sheela, N. Saswati, S. Ramakrisna, Biosorption of chromiumVI by free and immobilized *Rhizopus arrhizus*, Environ. Pollut. 104 (1999) 421.

[20] T.E. Abraham, Studies on enhancement of Cr(VI) biosorption by chemically modified biomass of *Rhizopus nigricans*, Water Res. 36 (2002) 1224.
[21] D. Kratochvil, P. Pimentel, B. Volesky, Removal of trivalent and hexavalent chromium by seaweed biosorbent, Environ. Sci. Technol. 32 (1998) 2693.
[22] D. Kratochvil, P. Pimentel, Advances in the biosorption of heavy metals, Trends Biotechnol. 16 (1998) 291.
[23] H. Ucun, Y.K. Bayhan, Y. Kaya, A. Chikici, O.F. Algur, Biosorption of chromium(VI) from aqueous solution by cone biomass of *Pinus sylvestris*, Bioresour. Technol. 85 (2002) 155.
[24] M. Kobya, Removal of Cr(VI) from aqueous solutions by adsorption onto hazelnut shell activated carbon: kinetic and equilibrium studies, Bioresour. Technol. 91 (2004) 317–321.
[25] N.K. Hamadi, X.D. Chen, M.M. Farid, M.G.Q. Lu, Adsorption kinetics for the removal of chromium(VI) from aqueous solution by adsorbents derived from used tyres and sawdust, Chem. Eng. J. 84 (2001) 95–105.
[26] G.J. Alaerts, V. Jitjaturant, P. Kelderman, Use of coconut shell based activated carbon for chromium(VI) removal, Water Sci. Technol. 21 (1989) 1701–1704.
[27] S. Babel, T.A. Kurniawan, Cr(VI) removal from synthetic wastewater using coconut shell charcoal and commercial activated carbon modified with oxidizing agents and/or chitosan, Chemosphere 54 (2000) 951–967.